UCL
Université
catholique
de Louvain

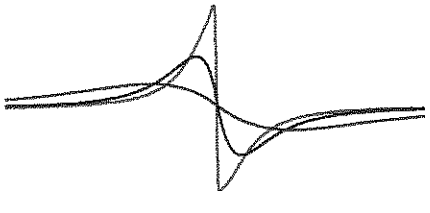

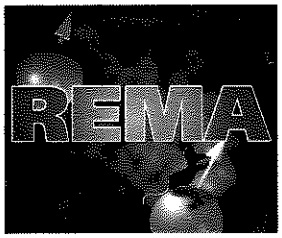

18th Meeting of the Benelux EPR Society

Brussels

June 1st, 2010

The organizers gratefully acknowledge the support of

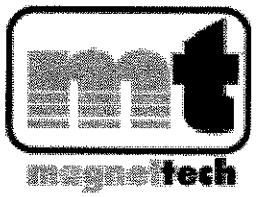

http://www.magnettech.de/

http://www.bruker-biospin.com/

In realizing this event

Programme

10.00	Registration of participants. Poster display. Coffee/Tea
10.30	*Bernard Gallez* (UCLouvain) Welcome
10.35-12.15	**Morning Session I**
	Chair: Sabine Van Van Doorslaer (University of Antwerpen)
10.35.	*M.A. Tarpan* (Ugent) Electron magnetic resonance study of primary free radicals in trehalose single crystals
11.00	*Y. Ling* (University of Antwerpen) EPR investigation of cationic radicals for organic electronic applications
11.25	*J. Leprince* (UCLouvain) Contribution of EPR technology to the study of dental resins
11.50.	*G. Mathies* (University of Leiden) CW EPR on Fe(III)-EDTA and Fe(III)-rubredoxin at 275 GHz using a single-mode cavity
12.15-13.00	Lunch (Buffet)
13.00-13.45	Poster Session
13.45-15.00	**Afternoon Session I**
	Chair: E. van Fassen (University of Utrecht)
13.45	*P.Y. Frapart* (Université Paris-Descartes) Taking care of metabolism in EPR *in vivo* imaging, a trithyl radical EPR study in mice articulation merged with X-Ray Micro CT
14.10	*P.H. Guelluy* (University of Liège) Multiple spectroscopic study of in vitro photodynamic therapy induced by PPME
14.35	*M. Ezhevskaya* (University of Antwerpen) B10 Phenylalanine plays a key role in neuroglobin
15.00	Coffee/Tea Break

15.20-16.35 Afternoon Session II

Chair: Peter Gast (University of Leiden)

15.20 *KAP. Wijnands* (University of Maastricht)
Intracellular NO metabolism by ESR and influence on endothelial dysfunction in a prolonged murine endotoxemia model

15.35 *M. Huber* (University of Leiden)
Distances between paramagnetic metal centers and spin labels in proteins by pulsed EPR: The RIDME method as a new tool.

16.00 *APD Nguyen* (KULeuven)
Point defects at the epitaxial Ge_3N_4/(111)Ge interface studied by electron spin resonance

16.25 General Assembly / Closing Remarks

16.35 Farewell drink

Poster presentations

P.1
S. Veriter et al (UCLouvain)
Can Mesenchymal Stem Cells Improve Early Neovascularization of Subcutaneous Encapsulated Islets?

P.2
E. Vinck et al (University of Antwerpen)
Unraveling the activation process of the cobalt Jacobsens's catalyst: A combined EPR-DFT approach

P.3
S. Zamani et al (University of Antwerpen)
Characterization of metal-doped and undoped titanium-oxide nanostructures as photocatalysts

P.4
K. Radermacher et al (UCLouvain)
Molecular NMR and EPR in vivo detection of cell death using specific phosphatidylserine-targeted iron oxide particles

P.5
S. Cambre et al (University of Antwerpen)
Endohedral copper(II)acetylacetonate/single-walled carbon nanotube hybrids characterized by Electron Paramagnetic Resonance

P.6
I.Lobysheva et al (UCLouvain)
EPR Assay of Superoxide Anion Production from Cardiovascular Tissues

P.7
B. Driesschaert et al (UCLouvain)
Chiral properties of stable Tetrathiatriarylmethyl radicals used for magnetic resonance applications

P.8
H. Moons et al (University of Antwerpen)
Electrically detected magnetic resonance (EDMR) on MDMO-PPV-based devices related to organic magnetoresistance (OMAR)

P.9
C. Diepart et al (UCLouvain)
MR characterization of the tumor microenvironment after arsenic trioxide treatment: evidence for an effect on oxygen consumption that radiosensitizes tumors

P.10
C. Diepart et al (UCLouvain)
Comparison of methods to measure oxygen consumption by tumor cells in vitro

P.11
N. Beziere et al (Université Paris Descartes)
Metabolic Stability of Cyclic Nitrone Adducts with $O_2^{\cdot-}$ And $^{\cdot}OH$ Towards Rat Liver Microsomes and Cytosol: a Stopped-Flow ESR Spectroscopy Study

P.12
Q. Godechal et al (UCLouvain)
Assessment of melanoma extent and melanoma metastases invasion by using Electron paramagnetic resonance and bioluminescence imaging

P.13
B. Jordan et al (UCLouvain)
Captopril and S-nitrosocaptopril as potent radiosensitizers: Comparative MR study and underlying mechanisms.

P.14
M. Shabestari et al (University of Leiden)
Monitoring Alzheimer amyloid peptide aggregation by EPR

P.15
O. Karroum et al (UCLouvain)
EPR study of the effect of Sorafenib on tumor hemodynamics: Potential use as a co-treatment for radiation therapy.

P.16
K. Keunen et al (KULeuven)
Intrinsic Si dangling bond defects at the (110)Si/SiO_2 interface

P.17
N. Kolbun et al (UCLouvain)
Experimental determination of the relative radial dose distribution in high gradient regions around iridium-192 wire source. Comparison between EPR Imaging, Gafchromic EBT film dosimetry and Monte Carlo simulations

P.18
D. Hebels et al (University of Maastricht)
Radical mechanisms in nitrosamine and nitrosamide-induced whole genome gene expression modulations in Caco-2 cells

P.19
P. Danhier et al (UCLouvain)
Potential role of PGE1 as a radiosensitizer: evaluation of the effect on tumor oxygenation using in vivo EPR oximetry

P.20
F. Desmet et al (University of Antwerpen)
EPR of the Cyanide Adducts of Protoglobin Mutants

Oral presentations

Electron magnetic resonance study of primary free radicals in trehalose single crystals

M.A. Tarpan[*a], H. De Cooman*[*b], E. Sagstuen[§] and F. Callens**

**Department of Solid State Sciences, Ghent University, Krijgslaan 281-S1,B-9000 Gent, Belgium*
[§] Department of Physics, University of Oslo, P.O. Box 1048 Blindern, N-0316 Oslo, Norway.
[a]Research Assistant and [b]Postdoctoral Fellow of the Flemish Research Foundation (FWO-Vlaanderen)

Radiation-induced radicals in sugars have recently gained considerable interest with respect to both fundamental and applied research. A number of studies are available that focus on the dosimetric characteristics of sugar systems. Other studies, like ours, aim to understand the identity and the structural properties of the involved radicals, and the radical reactions in which the primary or secondary products can be linked to the stable radicals.

Furthermore, carbohydrates represent extremely suitable model systems in which primary radiation-induced events may be studied. For instance, the detection of a trapped electron center in organic solids was first made in carbohydrate single crystals[1,2] and the nature of alkoxy radicals is readily investigated in these systems[3].

We present here experimental results obtained for low temperature radiation-induced radicals in trehalose single crystals. After 10 K *in situ* X-irradiation of trehalose single crystals four dominant radicals are present. Two radical species, labeled R1 and R2 are characterized by anisotropic g factors typical for the alkoxy type radicals. The R1 EPR spectrum is a broad singlet for most orientations, indicating only small proton hyperfine couplings. The direction of the maximum g value (g_{max}) indicates that O4' is the most likely site for the unpaired electron. R2 mainly exhibits a quartet EPR spectrum and the g_{max} direction favours O2 as the site of the unpaired electron. The other two radicals, R3 and R4, are characterized by a rather isotropic g tensor typical of alkyl radicals. R3 is characterized by a rather isotropic triplet in EPR which suggests two almost equivalent β proton hyperfine interactions. It is obtained by a net hydrogen abstraction from the C3' position. The second alkyl radical has most likely the unpaired electron localized at the C2 position.

A major purpose of this study is to compare the obtained results with the results reported by De Cooman et al[4] for 10 K X-irradiated sucrose single crystals. Trehalose and sucrose have a close structural similarity: they both are disaccharides composed of two units linked by a glycosidic oxygen bridge between their two anomeric carbon atoms, C1 and C1'. The study of very similar products may lead to a better general understanding of the radiation chemistry of carbohydrates.

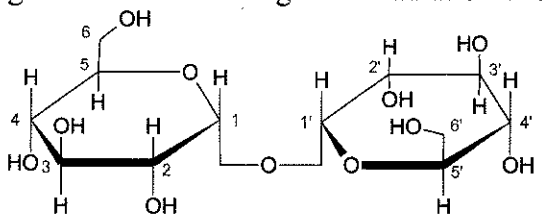

Chemical Structure of Trehalose

References

1. Box, H.C.; Budzinski, E.E.; Freund, H.G. J. Chem. Phys. 69 (1978), 1309
2. Box, H.C.; Budzinski, E.E.; Freund, H.G.; Potter, W.R. J. Chem. Phys. 70 (1979), 1320
3. Box, H.C.; Budzinski, E.E.; Freund, H.G. J. Chem. Phys. 81 (1984), 4898
4. De Cooman, H.; Pauwels, E.; Vrielinck,H.; Sagstuen,E.; Waroquier, M.; Callens, F. J. Phys. Chem. B 114 (2010), 666

EPR investigation of cationic radicals for organic electronics applications

Ling Yun[1], Hans Moons[1], Frank Blockhuys[2], C. Van Alsenoy[2], Etienne Goovaerts[1], Sabine Van Doorslaer1*

[1] *Department of Physics, University of Antwerp, 2610 Antwerp, Belgium*

yun.ling@ua.ac.be

[2]*Department of Chemistry, University of Antwerp, 2610 Antwerp, Belgium*

Poly(*p*-phenylene vinylene)-like (PPV-like) oligomers are found to be promising materials for the use as gas sensors, such as electronic noses. "Sensing" is done via the detection of changes in resistance of the active oligomer layer upon contact with the molecules of interest. However, in order to perform these conductimetric measurements, the PPV-like oligomers need to be oxidized, creating positive cations (polarons).

In this work, we present a combination of an X- and W-band continuous-wave and pulsed electron paramagnetic resonance (EPR) study and a DFT analysis of the material obtained after electrochemical oxidation of the sodium salt of *E,E*-2-(3-sulfopropoxy)-5-methoxy-1,4-bis[2-(2,4,6-trimethoxyphenyl)ethenyl]benzene (scheme).

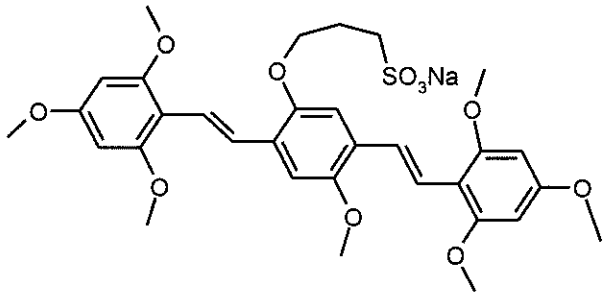

The W-band CW-EPR analysis allowed for the determination of the rhombic ***g*** tensor of the obtained paramagnetic species. As expected, the principal *g* values are similar to those obtained earlier for polarons formed by I_2-doping of PPV-type polymers.[1] Surprisingly, the X-band ENDOR and HYSCORE analysis revealed proton interactions with maximum couplings well below the ones detected previously in the polymers[1]. Since the polaron is extended over far more subunits in a polymer than in the oligomer under study (containing only three subunits), the inverse was expected, as corroborated by the DFT computations. Furthermore, the lack of a half-field signal in the CW-EPR spectra seems to exclude the formation of coupled polaron systems. Then in order to test the effect of different oxidation methods, the EPR spectra of polaron obtained via electrochemical oxidation and by chemical I_2 doping are compared and are found to differ. The characteristics of the oligomer polaron will be compared in detail to our earlier study on the I_2-induced polaron in the MDMO-PPV polymer. Furthermore, upon doping with I_2 for different times, we found an interesting dependence of the linewidth on doping time. This linewidth behaviour is now analyzed and compared to the one of electrochemically induced polarons. From combination of pulsed EPR measurements and solid-state NMR measurements (collaboration with R. Willem (VUB)) it could be shown that electrochemical treatment of the oligomers leads to ~99% oxidation with some magnetically isolated polaron sites. The signals change upon ageing due to stacking of un-oxidized and oxidized oligomers as is suggested by our DFT models. Quite good qualitative agreement between experiment and models could be obtained.

References

5. A Aguirre, P Gast, S. Orlinskii, I Akimoto, EJJ Groenen, H El Mkami, E Goovaerts & S Van Doorslaer; (2008) *Phys. Chem. Chem. Phys.* **10**, 7129-7138.

tooth reconstruction.

Contribution of EPR technology to the study of dental resins

Julian Leprince, Guillaume Lamblin, Jacques Devaux, Gaetane Leloup, Philippe Leveque, Bernard Gallez

School of Dental Medicine and Stomatology, Brussels, Belgium;
Institute of Condensed Matter and Nanosciences - Bio & Soft Matter (IMCN/BSMA), Université catholique de Louvain, Louvain-La-Neuve, Belgium;
Center for Research and Engineering in Biomaterials (CRIBIO), Brussels, Belgium;
Unité de résonance magnétique biomédicale, Louvain Drug Research Institute, Université catholique de Louvain, Brussels, Belgium.

In modern dentistry, photopolymerizable resin-based composites have become the choice material for the direct restoration of damaged teeth. These dimethacrylate-based materials set by radical polymerization, which leads to the entrapment of radical species inside the polymer network. These trapped radicals can be detected days or even months after photopolymerization by means of EPR spectroscopy. This unique feature of dental resins has enabled to take advantage of EPR technology to improve significantly the knowledge of dental resins. The present work will present an overview of how EPR technology significantly contributed to improve the understanding of dental resins and their setting process.

On the one hand, the results obtained shed new light on a new potential source of concern regarding biocompatibility. To start with, the follow-up of the signal intensity decrease in different environments highlighted the oxygen-dependance of free radicals long-term decay. Then, the use of two different spin-traps (EMPO[1] and DEPMPO[2]) produced evidence of ethoxy radical release by dental resins in ethanol. Further experiments demonstrated that hydroxyl radicals were firstly released from the methacrylated resin and secondly that they reacted with ethanol molecules to produce "secondary" ethoxy free radicals.

On the other hand, it was of prime interest to evaluate by EPR the amount of trapped radicals corresponding to various photoirradiation conditions parameters (light irradiance, irradiation time and radiant energy) for different material viscosities and filler content. There indeed exists a demand for reduction in curing exposure to minimize chairside procedure times, and in order to reach this time reduction, the general trend among manufacturers was to produce light curing units with increased irradiance. However, the impact of the different irradiation parameters on the reaction kinetics and final material properties was not clear, and the measurement of trapped free radicals gave new insights into the understanding of the photopolymerization. It notably revealed that the concentration of trapped free radicals significantly differed according to the curing protocol, as well as with resin viscosity and filler content.

Finally, a new approach using EPR imaging provided very interesting information on the spatial distribution of the free radicals, i.e. differences of trapped radical concentration in the thickness of the material depending on the curing time. Moreover, using spectral imaging, it was possible to compare the proportion of the two different radical species at different depths. Very interestingly, their respective proportions varied with curing depth, which provides new information on the local molecular mobility of the system.

[1] 5-ethoxycarbonyl-5-methyl-1-pyrroline N-oxide [2] 5-diethoxyphosphoryl 5-methyl-1-pyrrolyne N-oxide

How are you sure there are 2 spectral comp. inside?

CW EPR on Fe(III)-EDTA and Fe(III)-rubredoxin at 275 GHz using a single-mode cavity

G. Mathies[a], H. Blok[a], J.A.J.M. Disselhorst[a], P. Gast[a], H. van der Meer[a], D. Miedema[a], R. Almeida[b], J. Moura[b], W.R. Hagen[c] and E.J.J. Groenen[a]

[a)] Department of Molecular Physics, Universiteit Leiden, The Netherlands

[b)] Department of Chemistry, Universidade Nova de Lisboa, Portugal

[c)] Department of Biotechnology, TU Delft, The Netherlands

The study of the electronic structure of the active sites of metalloproteins can be greatly advanced by high-frequency/high-field (HF) EPR. Metalloproteins that have an iron atom in their active site have very short relaxation times and only CW EPR is feasible. The sensitivity and baseline stability of the CW HF EPR spectrometer must be very high for the following reasons. The amount of metalloprotein that is available for study is often limited and the same holds for the concentration. Also the HF EPR spectra cover large field ranges and the resonances can be very broad (1 T is no exception).

In 2003, we reported on the realization of a continuous-wave and pulsed EPR spectrometer operating at 275 GHz[1]. This spectrometer was equipped with a multifunctional single-mode cavity that allowed for optical access and ENDOR. With this cavity it is possible to measure CW EPR of paramagnetic species that have narrow resonances (for instance spin-labels), but the spectra of species that have broad resonances were poor. Therefore we developed a new single-mode cavity optimized for operation in CW mode.

We succeeded in measuring high quality spectra of frozen solutions with concentrations as low as 1 mM of the complex Fe(III)-EDTA (S = 5/2, zero field splitting parameter D = -22.6 GHz) and of the protein Fe(III)-rubredoxin (S = 5/2, D ≈ 45 GHz). This last spectrum spans more than 12 T (see the figure below). Analysis of these spectra allows for determination of the zero-field-splitting parameters and their strain. Spectra of rubredoxin from different organisms will be compared.

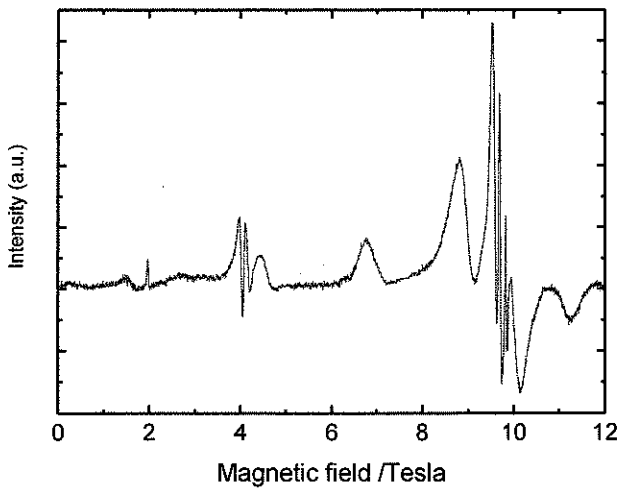

Figure: The 275 GHz CW EPR spectrum of 10 mM Fe(III)-rubredoxin from Desulfovibrio gigas acquired at 25 K.

[1]: H. Blok et al., J. Magn. Res. 166 (2004) 92-99

Taking care of metabolism in EPR *in vivo* imaging, a trithyl radical EPR study in mice articulation merged with X-Ray Micro CT.

Yves-Michel Frapart[a], Nicolas Bézière[a], Chrsitophe Decroos[a], Yun Xu-Lia, Fabienne Peyrot[a], Daniel Mansuy[a], Jean-Luc Boucher[a], Florence Cloppet[b]

a :Laboratoire de Chimie Biochimie Pharmacologiques et Toxicologiques, CNRS UMR 8601, Université Paris Descartes, 45, rue des Saints Pères, 75270 Paris Cedex 06, France
b :Laboratoire d'Informatique de Paris Descartes, Université Paris Descartes, 45, rue des Saints Pères, 75270 Paris Cedex 06, France

Yves.frapart@parisdescartes.fr

Free radicals (dioxygen, nitrioxide, reactive oxygen species …) play a key role in many biological processes , unfortunately their level and repartition in living body are still very hard to access. Electron Paramagnetic Resonance (with or without molecular probes such as spin traps) is well known as a cute spectroscopic method to study radicals. Since the late 90's, the way has been open to EPR imaging with mice imaging showing the repartition of dioxygen, nitric oxide, or endogenous radical such as melanin in mice. Radicals are short lived chemical species, even though spin trapped or specific radical have longer stability. The rapid disappearance of radicals especially in vivo is still an important parameter in such experiment. On the one hand such disappearance of the studied species during the image acquisition lead to artefacts, on the other hand it is a valuable information for the biologist . Here we used triArylMethyl molecular probes which has been used for oxymetry in mice articulation.

We take care of the disappearance of the radical, and gets its local pharmaco kinetic during image registration. This methodology is first proved on TEMPONE solution. And reconstructed a none correct image of the phantom.

We used X Ray micro tomograph to get the mice anatomy and fused and repositioned EPR Images and μCT images.

Finally this methods is applied on mice knee to developed a early diagnosis of articulation pathologies.

Lièpe Guelly

Multiple spectroscopic study of in vitro photodynamic therapy induced by PPME

Photodynamic therapy (PDT) emerges as an appropriated treatment to cure a multitude of oncological and non-oncological diseases. This curative technique combines the use of a photosensitizer (PS) as active molecule, a source of visible light in order to activate the PS and oxygenated pathologic tissues or cells as target. Pyropheophorbide-a-methyl ester (PPME), a derivative of Chlorophyll a, is a second-generation PS tested in PDT and a potential candidate for future clinical applications. The present study compares the improvement brings by a liposomal formulation of PPME versus free-PPME. A multitude of techniques have been performed in order to well characterize PPME in both ways of drug delivery. Among these techniques, we can list absorption and fluorescence microspectroscopies, confocal microscopy and FACS. The reactive oxygen species (ROS) produced after PPME-photoactivation have been identified by electron spin resonance combined with spin trapping technique. POBN spin trap has been chosen for its intracellular localization. In association with ethanol, this spin trap is normally specific to hydroxyl radical. Our results have however proven that the POBN/ethanol combination is also able to trap singlet oxygen. Competition experiments realized by specific ROS quenchers rendered possible the determination of the ROS-partition involved in the cellular death process induced by PPME.

B10 Phenylalanine plays a key role in neuroglobin

Maria Ezhevskaya[1], Florin Trandafir[1], Luc Moens[2], Sylvia Dewilde[2], Sabine Van Doorslaer[1]

[1] SIBAC Laboratory, University of Antwerp, Wilrijk, Belgium

[2] Department of Biomedical Sciences, University of Antwerp, Belgium

Discovered in 2000 human neuroglobin (NGB) still keeps the secret of its physiological role. Numerous studies made on NGB only speculated about its function. The neuronal location of NGB suggests a potential significance in neuroprotections during stroke. Several studies indicate that NGB plays a role in decreasing reactive oxygen species (ROS) and reactive nitrogen species (RNS).

In this work, we use EPR spectroscopy to show that the PheB10 residue plays an essential role. For that aim Phe at B10 position was mutated to a Leu residue.

X-band CW measurements at low-temperature on samples with and without Phe at the B10 position revealed a significant difference of the low-field g_z component of low-spin ferric NGB. As known from earlier work a disulfide bridge can be formed between Cys CD7 and D5, which has a marked influence on the heme environment. This results in the fact that the EPR spectra of the ferric form of wt NGB with ($NGB_{S\text{-}S}$) and without (NGB_{SH}) disulfide bridge differ clearly. The low-field component of ferric B10Leu NGB is shifted down-field from the one of the wt NGB_{SH} contribution. In contrast to ferric wt NGB, the low-field EPR signal of ferric B10Leu NGB is not split in two, indicating that there is little or no variation in the heme-pocket region upon formation of the disulfide bridge. Moreover, addition of DTT to the B10Leu NGB variant reveals only a very small shift of the g_z component of the EPR signal.

Both EPR and optical absorption spectroscopy experiments have been performed to map out the reaction of H_2O_2 with NGB. While a 1:1 wt NGB:H_2O_2 ratio do not change the EPR signal, addition of a 100-fold excess of H_2O_2 to wt NGB leads to a reduction of the EPR contribution of the ferric form. In addition, a small shift to higher wavelengths is observed in the absorption spectra suggesting a small formation of the ferryl form of the heme. Ferric B10Leu NGB is much more easily oxidized by H_2O_2. Furthermore, upon addition of H_2O_2 to ferric wt NGB and ferric B10Leu NGB, the EPR signature of a radical appears in the EPR spectra.

Room-temperature EPR experiments with H_2O_2 have been performed to test the radical formation reactions by use of a DMPO spin trap. We see a clear decrease in the DMPO-$^{\bullet}$OH EPR signal upon increase of the NGB concentration. In contrast, this effect is not found for the B10Leu NGB or myoglobin.

Intracellular NO metabolism by ESR and influence on endothelial dysfunction in a prolonged murine endotoxemia model

KAP. Wijnands, JJ. Briéde, E. van Faassen, WA. Buurman, WH. Lamers, H. Vink, M. Poeze

Objective: Endotoxemia results in a decreased microcirculatory flow, accompanied glycocalyx degradation and endothelial dysfunction. The function of glycocalyx, a network of membrane-bound proteoglycans and glycoproteins, covering the endothelium luminally, determines Nitric Oxide (NO)-dependent vascular function, and vascular permeability.
NO and citrulline (CIT) are produced from arginine (ARG), by Nitric Oxide synthases (NOS). CIT can be recycled back to ARG by the enzyme Argininosuccinate synthase (AS) in the kidney and endothelium. Metabolic pathways of ARG-NO metabolism in human sepsis are characterized by a decreased arginine *de novo* synthesis and increased ARG breakdown by arginase. Furthermore, the inflammatory NOS (iNOS) is upregulated during endotoxemia and sepsis, reducing the available extracellular ARG to produce NO leading to decreased ARG availability for NO synthesis by the endothelial NOS (eNOS), resulting in accompanied endothelial dysfunction and glycocalyx degradation.
Previous experimental studies with acute bolus injection of endotoxin did not result in decreased arginine *de novo* synthesis, making it a less appropriate model to study human metabolic arginine-NO disorders in sepsis. Therefore, there is a need to develop a prolonged endotoxin model to study these intracellular arginine – NO disturbances which underlie endothelial dysfunction.
Aim: To investigate the effect of a prolonged endotoxic insult on the intracellular NO metabolism and endothelial dysfunction.
Methods: Mice received a continuous intravenous endotoxin (LPS, 200 µg total) or sterile saline infusion for 18 hrs. Endogenous NO levels were determined by *in vivo* NO spin trapping (30 min) with Fe-DETC complexes. After NO trapping, the animals were sacrificed, arterial blood sampled and tissues snap frozen in liquid nitrogen. The trapping yield of the nitrosyl-Fe^{2+}-DETC complex (MNIC) in tissues was quantified at 77 Kelvin by comparison with calibrated reference solutions. Amino acid concentrations in plasma tissue? were measured with High Performance Liquid Chromatography. Side stream dark field imaging, a stroboscopic LED ring-based imaging modality, was used to evaluate the glycocalyx, by measuring the .
Results:
Tissues of LPS-treated mice showed 2-3 fold higher MNIC in all tissues tested (kidney, liver, heart, jejunum) compared to control mice. In this prolonged model, the MNIC yields are significantly lower than in typical murine acute sepsis models, where the LPS is administered as bolus injection.
As detected with ESR, whole blood of LPS challenged mice contained significant quantities of MNIC (0.35 mM), as well as nitrosyl-Hb complexes.
Plasma arginine and citrulline concentrations of LPS challenged mice were significantly lower than in controls. In contrast, plasma ornithine levels were significantly higher.
The red blood cell diameter in the LPS group was significantly larger (average difference of 0,3µm, $p < 0.05$) compared to the control group, indicating increased glycocalyx degradation
Immunohistochemistry showed significantly increased positive MPO staining in the gut compared to control animals.
Conclusion:
Prolonged infusion of LPS has reproducible effects on the NO levels and arginine-citrulline metabolism in both blood and tissue compartments. Enhanced endogenous NO levels, as detected by ESR, are correlated with decreased plasma levels of the precursor arginine and citrulline and results in glycocalyx degradation with associate endothelial leakage.
Our murine model with prolonged infusion appears applicable to the human clinical situation to study the arginine - NO metabolism of sepsis.

Distances between paramagnetic metal centers and spin labels in proteins by pulsed EPR: The RIDME method as a new tool.

Sergey Milikisyants [a], *Francesco Scarpell* [a], *Michela Finiguerra* [a,b], *Marcellus Ubbink* [b]

Martina Huber [a]

Department of Molecular Physics [a] **and Leiden Institute of Chemistry** [b], **Leiden University, Postbox 9504, 2300 RA Leiden, The Netherlands**

Structure determination related to biological systems is increasingly done by pulsed EPR, where the potential to measure nm distances between spin labels has paved the way even towards structure determination by triangulation.[1]

Fig. 1.

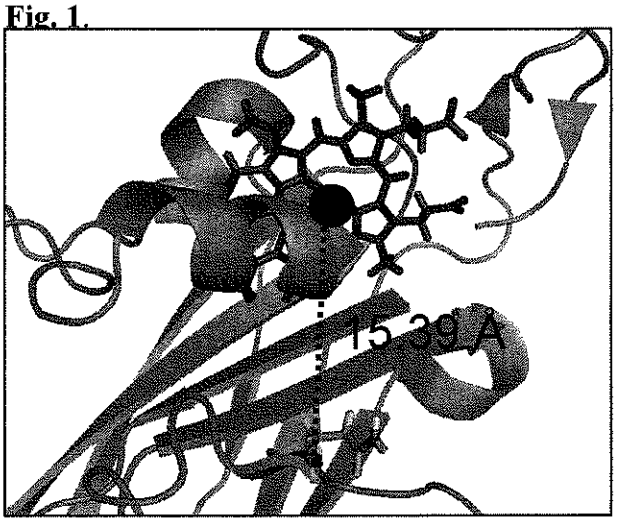

Transition metal ion centers abound in protein systems (e.g. Fig. 1), but their potential as markers for distance determination has been limited by their large g-anisotropies and fast relaxation times. For many of these centers, pulse sequences that directly target the dipolar interactions cannot be applied because the excitation bandwidth is not sufficient to cover a substantial part of the EPR spectrum of such centers. The RIDME method[2] circumvents this problem by making use of the spin-lattice relaxation (T_1)-induced spin-flip of the transition-metal ion. Designed to measure distance between such a fast relaxing metal center and a radical, it suffers from a dead time problem. This disadvantage can be avoided by the five-pulse RIDME (5p-RIDME) sequence (Fig. 2)[3].

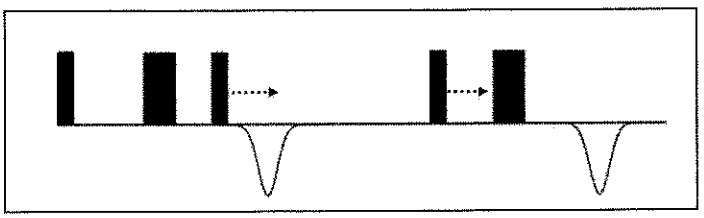

Fig. 2

We apply this method to measure the distance between a low-spin Fe(III) center and a spin label in spin-labeled *cytochrome f* . Fig. 1 shows the location structure of the protein and the and the of the spin label (bottom of Fig.) metal center (blue). The complete dipolar trace was obtained, yielding the distance expected from the structure[3].

References

1. Hilger, D et al. *Biophysical Journal* **2007**, *93*, 3675-3683l, Bhatnagar, J et al. *Two-Component Signaling Systems, Pt B* **2007**, *423*, 117-133.
2. L.V.Kulik, et al. J. Magn. Res. **2002**, *157* , 61-68
3. S. Milikisyamts J. Magn. Res. **2009**, *201*, 48-56.

Point defects at the epitaxial Ge_3N_4/(111)Ge interface studied by electron spin resonance

A. P. D. Nguyen, V.V. Afanas'ev, and A. Stesmans.

Department of Physics and Astronomy, University of Leuven

Celestijnenlaan 200D, 3001 Leuven, Belgium

Because of its higher bulk electron and hole mobilities over Si, germanium has regained technological interest for application in future generations of CMOS devices with the potential of realizing faster devices, together with reduced power consumption enabled by the smaller bandgap. But for whatever semiconductor envisioned for technological implementation, the availability of an appropriate insulator is essential. In this respect, a most crucial requirement for any functional MOS entity is ensuring a sufficiently low density of detrimental traps (defects) down to the (sub) $10^{10}cm^{-2}$ level at the semiconductor/gate insulator interface.

Recently, it has been shown that, under application of a very high O_2-presure, a Ge/GeO_2 interface can be realized [1] with relative low interface defect density (D_{it} □ 3×10^{11} $cm^{-2}eV$). Unfortunately, the common Ge oxide cannot be used as insulator material because of its thermodynamic unstability. Application of some other oxides, such as HfO_2, was not found successful because of a high density of interface defects [2]. Yet, as another possibility, germanium nitride is considered as a potential gate insulator, due to its high dielectric constant, good thermal stability, and possible implementation compatible with the low temperature Ge fabrication process. Theoretically, the mismatch between epi-Ge_3N_4 and (111)Ge is less than 2.5 % with no formation of interface defects. However, there is still a lack of insight regarding inherent defects occurring in this structure.

In this work, the electron spin resonance (ESR) technique has been used to investigate paramagnetic defects at the interface of epitaxially grown Ge_3N_4/(111)Ge entities with nm-thin Ge_3N_4 layers, studied here as a promising structure. No $^{\bullet}Ge{\equiv}Ge_3$ (Ge P_b-type) dangling bond centers could be observed. Yet, as sole signal, there appears an anisotropic center (areal density $<10^{12}$ cm^{-2}) of axial symmetry, characterized by $g_{//}\sim2.0032$ and $g_{\perp}\sim2.0023$, most prominently after VUV excitation. Based on comparison of its specific ESR properties with previous theoretical results, the defect is suggested to concern the Ge K-type center. The properties and nature of the center are discussed within the epitaxial nature of the interface.

[1] CH. Lee, T. Tabata, T. Nishimura, et al. Appl. Phys. Express **2**, 071404 (2009)

[2] H. Kim, P.C. McIntyre, C.O. Chui, et al. App. Phys. Lett. **85**, 2902 (2004)

Modulation frequency?

Poster presentations

Can Mesenchymal Stem Cells Improve Early Neovascularization of Subcutaneous Encapsulated Islets?

Sophie Veriter[1], Najima Aouassar[1], Marie-Sophie. Paridaens[1], Charlotte Stuckmann[1], Pierre-Yves Adnet[1], Bénédicte Jordan[2], Bernard Gallez[2], Pierre Gianello[1], Denis Dufrane[1]

[1] Université catholique de Louvain, Faculty of Medicine, Experimental Surgery, Brussels, Belgium

[2] Université catholique de Louvain, Faculty of Medicine, Biomedical Magnetic Resonance, Brussels, Belgium

Introduction

Although 5 % of O_2 are present in alginate (high M) encapsulated pig islets (transplanted in the subcutaneous tissue (SC) of non-diabetic rats), a mean of 30% of islets are lost during the first week post-transplantation. This oxygen stress could be increased by micro/macrovascular lesions due to the diabetes. Therefore, we investigated, both *in vitro* and *in vivo*, the potential of mesenchymal (bone marrow (BM-MSC) and adipose (AMSC)) stem cells to improve angiogenesis, islet survival and diabetes correction.

Materials and Methods

(i) Oxygen pressures (pO_2) inside SC high-M 3% v/v implants were weekly compared *in vivo* in healty and streptozotocin (STZ)-induced diabetic rats (n=16) by Electronic Paramagnetic Resonance (EPR) up to 4 weeks post-transplantation. After graft explantation, neoangiogenesis surrounding implant and number of cells expressing Vascular Endothelial Growth Factor (VEGF) were assessed by histomorphometry.

(ii) The impact of islets transplantation on implant oxygenation was evaluated by pO_2 measurements by EPR and quantification of vessels/VEGF positive cells surrounding encapsulated pig islets implanted SC in STZ-induced diabetic and non diabetic rats (n=14).

(iii) Proangiogenic properties of BM-MSC and AMSC in normoxic and hypoxic conditions were assessed *in vitro* by incubation at 0.1, 3, 5 and 21% O_2 for 24, 48 and 72hr. MSC (BM and adipose) viability was determined by MTT test and the release of VEGF was quantified by ELISA.

(iv) The proangiogenic properties of stem cells were assessed *in vivo* by pO_2 measurements by EPR inside AMSC encapsulated in high-M alginate compared to empty capsules implanted SC in diabetic rats (n=2x9).

The statistical t-student and ANOVA tests were performed to compare the experimental groups.

Results

(i) A significant higher pO_2 was found in alginate implants of non-diabetic vs. diabetic rats (4.32 ± 1.05 vs 3.42 ± 0.65 % O_2, respectively; p=0.038) at 1 week post-implantation. However, similar pO_2 were measured in both groups at 2/3/4 weeks (3.29 ± 0.13 % O_2). A higher number of cells expressing VEGF (p=0.033) surrounding the implant was found for non-diabetic vs. diabetic rats.

(ii) The presence of islets reduces implants pO_2 in comparison to empty islets (2.31 ± 1.75 vs. 4.32 ± 1.05 % O_2 for non-diabetics and 2.36 ± 0.82 vs. 3.42 ± 0.65 % O_2 for diabetic rats ($p<0.05$)). A higher number of cells expressing VEGF was found when islets were implanted ($p<0.05$).

(iii) Hypoxia did not affect MSC (BM and adipose) viability. BM-MSC released more VEGF in hypoxia than in normoxic conditions ($p<0.05$). In contrast, VEGF released by AMSC was similar in the different culture conditions with a significant higher level of VEGF released by AMSC than BM-MSC (11,274 ± 679 vs. 2,364 ± 94 pg/ml, respectively; $p<0.001$).

(iv) *In vivo*, higher oxygenation levels were observed in implants containing AMSC than in empty implants (AUC 11.46 ± 2.55 vs. 9.40 ± 0.48 % O_2.week). A higher number of vessels and VEGF-positive cells surrounding these latest implants were observed in comparison to empty implants ($p<0.01$).

To study the beneficial properties of AMSC in a pre-clinical model, two diabetic monkeys were grafted SC with porcine islets co-encapsulated with AMSC 5 weeks ago and diabetes is currently corrected (in course).

Conclusions

Diabetes induces a delay of implant oxygenation as well as a reduction of VEGF expression. Implantation of islets decreases also implant oxygenation. BM-MSC and AMSC can release VEGF in moderate hypoxia (5% O_2). AMSC improve the *in vivo* oxygenation of encapsulated islets placed SC, limiting therefore the lost of islets after transplantation.

Unraveling the activation process of the cobalt Jacobsen's catalyst: A combined EPR-DFT approach

Evi Vinck[1], Sabine Van Doorslaer[1], Damien M. Murphy[2], and Ian A. Fallis[2].

[1]*University of Antwerp, Department of Physics, Universiteitsplein 1, 2610 Wilrijk, Belgium*
[2]*Cardiff University, Department of Chemistry, Cardiff CF10 3TB, Wales, UK*

In this work, the activation process of the metal salen catalyst *N,N'*-Bis(3,5-di-tert-butylsalicylidene)-1,2-cyclohexanediamino cobalt^{II} ([Co(**1**)]) has been studied using a combined electron paramagnetic resonance (EPR) – density functional theory (DFT) approach. The [Co(**1**)] catalyst is activated by the addition of acetic acid and subsequent exposure to air. The resulting complex is widely used to separate the enantiomers in racemic mixtures of terminal epoxides via a hydrolytic kinetic resolution (HKR) reaction. Despite its widespread use, the nature of the activated species is still poorly understood.

The CW-EPR data, performed in this work, show that different molecules are formed upon activation of the catalyst, including a cobalt-bound phenoxyl radical, situated on ligand **(1)**. It is the first time that such a species is observed. Detailed information on the electronic structure of the different species that are formed upon activation, including the phenoxyl radical was obtained using pulsed-EPR techniques, such as the four-pulse ESEEM technique HYSCORE (hyperfine sublevel correlation). The EPR data are complemented with density functional theory (DFT) computations, which corroborate that a stable phenoxyl radical can be formed on the salen ligand.

Characterization of metal-doped and undoped titanium-oxide nanostructures as photocatalysts

Sepideh Zamani*, .Ignacio Caretti*, Evi Beyers **, Stefan Ribbens**, Pegie Cool**, Sabine Van Doorslaer*

*University of Antwerp, Department of Physics, Laboratory of SIBAC, Universiteitsplein 1, 2610 Wilrijk, Belgium
** University of Antwerp, Department of Chemistry, Laboratory of Adsorption and Catalysis, Universiteitsplein 1, 2610 Wilrijk, Belgium.

The semiconductor titanium dioxide (TiO_2) materials have been investigated over the last three decades due to their photocatalytic activities. The morphology and high surface areas of these materials are responsible for their high efficiency in catalysis. Some of the applications of these materials are, self-cleaning building materials, solar sells, etc. Here, H-tube materials (tube-like TiO_2) are doped with different transition metals, such as vanadium and copper ions, using the MDD method. The doping is targeted at improving the catalytic properties of the material and at the reduction of the band gap, which lies in the UV range for the undoped material. In the second part of this work, we will focus on the EPR study of these materials at different temperatures under UV and visible light irradiation. In this way, information about the photo-induced charge separation is obtained.

MOLECULAR NMR AND EPR IN VIVO DETECTION OF CELL DEATH USING SPECIFIC PHOSPHATIDYLSERINE-TARGETED IRON OXIDE PARTICLES.

Kim A. Radermacher[1], S. Boutry[2], S. Laurent[2], L. Vander Elst[2], I. Mahieu[2], C. Bouzin[3], J. Magat[1], V. Gregoire[4], O. Feron[3], R.N. Muller[2], B.F. Jordan[1], and Bernard Gallez[1].

[1]Biomedical Magnetic Resonance Unit, Louvain Drug Research Institute, Catholic University of Louvain (UCL), Avenue E. Mounier 73/40, 1200 Brussels, Belgium.

[2]NMR and Molecular Imaging Laboratory, University of Mons, Belgium.

[3]Unit of Pharmacology and Therapeutics, UCL, Belgium.

[4]Center for Molecular Imaging and Experimental Radiotherapy, UCL, Belgium.

Purpose:

The aim of the study was to develop a new molecular marker for non invasive diagnosis and monitoring of cell death in order to evaluate the efficacy of anti-cancer treatments in vivo. The phosphatidylserine-targeted peptide E3, isolated by phage-display (1), was coupled to pegylated ultrasmall particles of iron oxide (USPIO). USPIO particles are used as negative contrast agent for magnetic resonance imaging (MRI) due to strong T2 and T2* effects and besides this method they can also be quantitatively detected by electron paramagnetic resonance (EPR) (2).

Methods and Results:

Transplantable liver tumors (TLT) were implanted in the gastrocnemius muscle of NMRI mice and tumor cell death was induced by x-ray irradiation. Accumulation of the intravenously administered USPIO-E3 particles in treated and untreated TLT tumors was compared to the accumulation of control particles (ungrafted USPIO and USPIO grafted to a scrambled peptide) ex vivo by X- band EPR, and in vivo by L-band EPR and by T2-weighted MRI. In irradiated tumors was greater accumulation of targeted USPIO particles compared to control particles or compared to accumulation of targeted particles in untreated tissues. MRI and X-band EPR were also used to compare accumulation of USPIO-E3 in 3 different tumor models presenting different degrees of radiosensitivity (fibrosarcoma FsaII is less sensitive than hepatocarcinoma TLT which is less sensitive than lymphoma EL4) in order to evaluate the ability of this new biomarker to distinguish between different levels of tumor celldeath.

Conclusion:

The major finding of the present investigation is that functionalization of the surface of iron oxide particles with the E3 hexapeptide allows the sensitive detection and mapping of tumor cell death after cytotoxic treatment. This molecular targeted system should be evaluated further as a potential biomarker of tumor response to treatment.

Référence: (1) Laumonier C. et al. J. Biomol. Screen. 2006;11:537-545.
(2) Ianonne A. et al. Invest. Radiol. 1992;27:450-455.

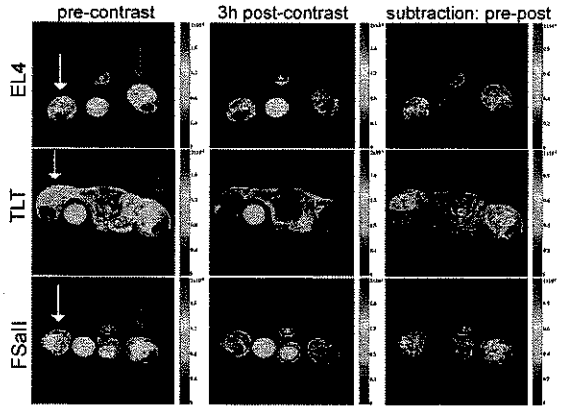

Figure: Axial images of different tumor models as obtained by T2-weighted MRI. The red arrow indicates the irradiated tumor (right paw) and the white arrow the untreated control tumor (left paw).

Endohedral copper(II)acetylacetonate/single-walled carbon nanotube hybrids characterized by Electron Paramagnetic Resonance

Sofie Cambré, Wim Wenseleers and Etienne Goovaerts

Experimental Condensed Matter Physics Laboratory, University of Antwerp, Universiteitsplein 1, 2610 Antwerp (Belgium)

The encapsulation of organometallic paramagnetic molecules, copper(II) acetylacetonate ($Cu(acac)_2$), inside single walled carbon nanotubes (SW CNTs) is studied using continuous wave electron paramagnetic resonance (EPR).[1] By preparing samples from either fully opened or closed SW CNTs[2], the EPR spectra of encapsulated and non-encapsulated molecules can be clearly identified. The EPR spectrum originating from the encapsulated molecules is unchanged by dispersion of the endohedral nanohybrids in a solvent or by solubilization of the nanohybrids in water using bile salt surfactants[3], demonstrating that the CNTs protect the encapsulated molecules from changes in the external environment. The EPR parameters obtained for the encapsulated molecules show that these molecules experience an extremely apolar environment. From the EPR spectra of the encapsulated molecules the distances between the encapsulated molecules inside the CNTs can be estimated by adapting Van Vleck's method of moments[4] for the case of a one-dimensional array of molecules. Furthermore, orientation dependent EPR experiments in combination with polarized Raman scattering experiments of preferentially aligned endohedral CNT hybrids inside stretched polymer film samples, yield information on the orientational distribution of the encapsulated molecules inside the SW CNTs.

(1) Cambre, S.; Wenseleers, W.; Goovaerts, E., *J. Phys. Chem. C* **2009**, *113*, 13505-13514.
(2) Wenseleers, W.; Cambre, S.; Culin, J.; Bouwen, A.; Goovaerts, E., *Adv. Mater.* **2007**, *19*, 2274-+.
(3) Wenseleers, W.; Vlasov, I. I.; Goovaerts, E.; Obraztsova, E. D.; Lobach, A. S.; Bouwen, A., *Adv. Func. Mater.* **2004**, *14*, 1105-1112.
(4) Van Vleck, J. H., *Phys. Rev.* **1948**, *74*, 1168.

EPR Assay of Superoxide Anion Production from Cardiovascular Tissues.

Irina Lobysheva, Joanna Hammond, Tim Van Assche, Bernard Gallez, and Jean-Luc Balligand
University of Louvain Medical School, avn. E. Mounier, 52, B-1200 Brussels BELGIUM
Irina.Lobysheva@uclouvain.be

Reactive oxygen species (ROS), generated by NOX enzymes or uncoupling of eNOS and mitochondria play an important role in physiological regulation and also involved in pathophysiological processes underlying cardiovascular diseases such as inflammation, hypertrophy, and remodeling of vessels and cardiac tissue. But analytical distinction between different type of ROS, local subcellular formation and quantitative assay in cells and biological tissues is still problematic due to low concentration, short life-time and high chemical activity of ROS.

Detection of superoxide anions by EPR spin trapping was developed and successfully applied during last decades. We analyzed properties of several cyclic hydroxylamines, known as $O_2^{-\cdot}$ spin probes with different sensitivity and lipophility (CMH, CPH and CAT1H) in suspension of endothelial cells, isolated aortic rings and dissected heart tissues stimulated for NOX activation or not. This compounds can form stable paramagnetic adduct (nitroxide, A_N = 16.1 G) after oxidation by $O_2^{-\cdot}$ or peroxynitrite. We have found very high and SOD-dependent sensitivity of all tested spin probes in cell-free $O_2^{-\cdot}$ generating system with xanthine/xanthine oxidase (CMH > CPH > CAT1H), but abnormal sensitivity of CPH to SOD in this condition. SOD decreased CPH autoxidation in absence of any $O_2^{-\cdot}$ production by ~2.5 times. The last effect was not found for CMH and CAT1H.

We observed in biological samples:

1. Good sensitivity of CMH spin probe for detection of basal and stimulated radical formation from cultured endothelial cells and tissues (aortic rings and dissected heart tissues) when EPR signal was monitored after in situ stimulation at 37°C. But basal and stimulated signals were hardly inhibited by SOD and PEG-SOD in tissue and cells.
2. Radical formation with CAT1H and CPH in isolated aortas and endothelial cells (HUVECs), on the contrary, was strongly inhibited by SOD (after 2-4 hours of preincubation) due to low lipophility of these spin probes and preferential extracellular detection of radical.
3. ROS production was found increased after Angiotensin II stimulation (2 μmol/L, 4 h.) from 0.67 to 1.43 pmol/min/mg of dry tissue in isolated aortas (monitoring at 37°C).
4. Interestingly, that addition of uric acid (500 uM) partly inhibited radical formation stimulated by Angiotensin II in HUVECs, but did not interact with basal cell radical production.

Taken together, these results demonstrate good applicability of the EPR spin monitoring technique to biological studies of $O_2^{-\cdot}$ generation. Spin probe CAT1H was found as the easiest to handle, but the effect of SOD or other ROS scavengers have to be tested to ascertain the type of formed radicals. Additional study of SOD effects and SOD loading into tissue and cells is necessary for proper utilization of CMH and CPH.

CHIRAL PROPERTIES OF STABLE TETRATHIATRIARYLMETHYL RADICALS USED FOR MAGNETIC RESONANCE APPLICATIONS

Benoît Driesschaert[a,b], Raphaël Robiette[a], Bernard Gallez[b,*], Jacqueline Marchand-Brynaert[a,*]

[a]Institute of Condensed Matter and Nanosciences (IMCN), Molecules, Solids and Reactivity (MOST), Université catholique de Louvain, UCL, place Louis Pasteur 1, B-1348 Louvain-la-Neuve, Belgium, [b]Louvain Drug Research Institute (LDRI), Biomedical Magnetic Resonance Section, Université catholique de Louvain, UCL, avenue Mounier 73.40, B-1200 Bruxelles, Belgium.

jacqueline.marchand@uclouvain.be ; bernard.gallez@uclouvain.be

Tetrathiatriarylmethyl radicals (Fig. 1) are a family of versatile stable radicals used in dynamic nuclear polarization (DNP) and in electron paramagnetic resonance (EPR) spectroscopy/imaging for a number of applications. The chemistry of these compounds is currently under development in dedicated laboratories. Modifications are carried out for improving the performance and extending the variety of applications. Dendritic trityl radicals have been synthesized to enhance their stability,[1] fluorinated ones to assay tumor oxygenation with high sensitivity using perfluorocarbon formulations,[2] trityl-nitroxide biradicals for the simultaneous measurement of redox status and oxygenation,[3] amino derivatives for dual pH/oxygen assessment,[4] etc.

Tetrathiatriarylmethyl compounds adopt a propeller-like conformation in which all rings have the same direction of twist (Fig.1).[5] Right-handed or left-handed helices feature an enantiomeric relationship. This stereoisomerism may have important consequences if a chiral group is connected to the trityl, because it may result in the formation of diatereoisomers with possibly different chemical, physical and biological properties. In this work, we report experimental and theoretical studies of the stereoisomerization of such compounds.

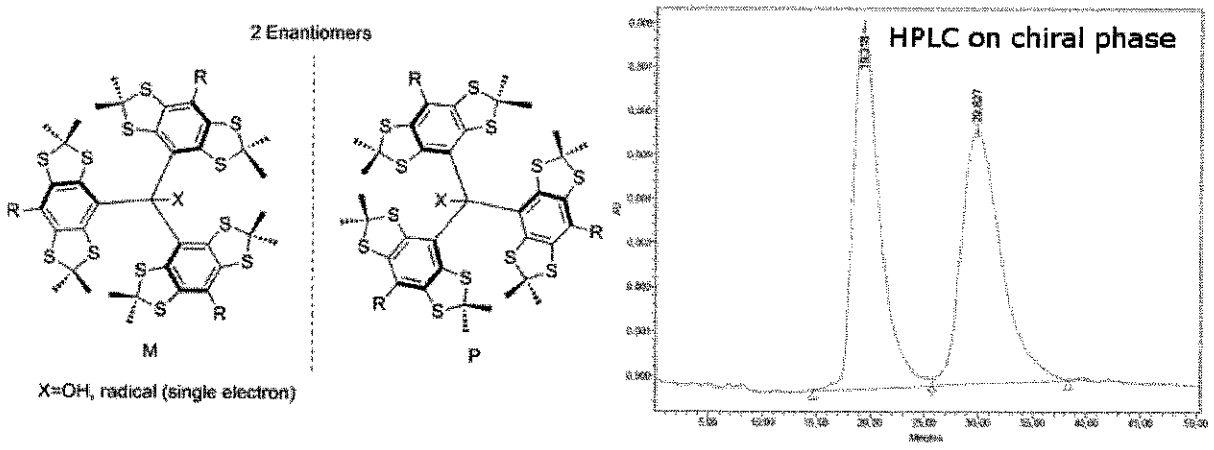

Figure 1.

(1) Liu, Y.; Villamena, F. A.; Zweier, J. L. *Chem. Commun.* **2008**, 4336-4338. (2a) Driesschaert, B.; Charlier, N.; Gallez, B.; Marchand-Brynaert, J. *Bioorg. Med. Chem. Lett.* **2008**, 18, 4291-4293. (2b) Charlier, N.; Driesschaert, B.; Wauthoz, N.; Beghein, N.; Préat, V.; Amighi, K.; Marchand-Brynaert, J.; Gallez, B. *J. Magn. Reson.* **2009**, 197, 176-180. (3) Liu, Y.; Villamena, F. A.; Rockenbauer, A.; Zweier, J. L. *Chem. Commun.* **2010**, 46, 628-630. (4) Dhimitruka, I.; Bobko, A. A.; Hadad, C. M.; Zweier, J. L.; Khramtsov, V. V. *J. Am. Chem. Soc.* **2008**, 130, 10780-10787. (5) Bowman, M. K.; Mailer, C.; Halpern, H. J. *J. Magn. Reson.* **2005**, 172, 254-267.

Electrically detected magnetic resonance (EDMR) on MDMO-PPV-based devices related to organic magnetoresistance (OMAR)

Hans Moons[*], *Francisco Bloom*[#], *Bert Koopmans*[#], *Etienne Goovaerts*[*]

[*] *ECM Laboratory - Department of Physics, University of Antwerp, Belgium*
[#] *Ctr Nanomat - Department of Applied Physics, University of Technology, Eindhoven, Netherlands*

Recently, the magnetic field effect of organic magnetoresistance was discovered.[1] When a small magnetic field is applied to an organic semiconductor film, the electrical resistance can be changed by about 10 per cent. This unusual change in conductivity is promising with regard to future applications, but the physics behind is yet not well understood. In this work we present the results of electrically detected magnetic resonance on MDMO-PPV-based devices. MDMO-PPV is the workhorse polymer in organic electronics and is in this case sandwiched between an aluminum electrode and an ITO electrode accommodated with a LiF and a PEDOT:PSS layer for better electron and hole injection, respectively. The influence of microwaves (9.4 GHz) on the conductivity of the device at a certain magnetic field is measured. Below a certain threshold bias voltage, only one resonant signal can be detected. However, above this threshold voltage, the initial signal reverses sign and a second resonant signal is observed. A similar transition from decrease to increase of conductivity is observed in the OMAR experiments at the same voltage. This threshold corresponds with the onset of bipolar transport confirmed by the I-V characteristics.[2] EDMR on unipolar devices, where either only electrons or only holes are injected, indicate that the two signals, noticed in the EDMR experiments on bipolar devices, result from separate contributions from each of the charge carriers, i.e. holes and electrons. These experiments support the hypothesis[3] that bipolaron formation is responsible for the increase/decrease of the resistance as a function of the magnetic field in the device.

1. Francis T.L. et al., New journal of Physics, 6 (2004) 185
2. Bloom F.L. et al., Applied Physics Letters,93 (2008) 263302
3. Wagemans W. et al., Journal of Applied Physics, 103 (2008) 07F303

MR CHARACTERIZATION OF THE TUMOR MICROENVIRONMENT AFTER ARSENIC TRIOXIDE TREATMENT: EVIDENCE FOR AN EFFECT ON OXYGEN CONSUMPTION THAT RADIOSSENSITIZES SOLID TUMORS

Caroline Diepart[1], Bénédicte F.Jordan[1], and Bernard Gallez[1]
1: Laboratory of Biomedical Magnetic Resonance, Université catholique de Louvain,
Avenue Mounier 73, B-1200 Brussels, Belgium

Introduction

The partial pressure of oxygen (pO_2) is a crucial factor affecting the response of tumors to irradiation and other cytotoxic treatments. It has been predicted that modification of oxygen consumption is much more efficient at alleviating hypoxia than modification of oxygen delivery.

Arsenic has been reported to have anti-tumor effect in acute promyelocytic leukemia and in solid tumors. As_2O_3 seems also to inhibit mitochondrial respiratory function in human leukemia cells. Thus, we hypothesized that As_2O_3 could be an important modulator of tumor oxygenation by affecting the oxygen consumption of tumors. We characterize the evolution of the tumor micro-environment after As_2O_3 treatment.

Materials and methods

The effect of As_2O_3 (5 mg/kg) was studied in a transplantable liver tumor model (TLT) and in a Lewis Lung Carcinoma (LLC). Local pO_2 was measured in vivo using low frequency EPR (1) and ^{19}F-relaxometry (2). The oxygen consumption rate was measured in vitro using high-frequency EPR. At the maximum pO_2 (after 1h30) perfusion and radiation sensitivity were also studied by Patent Blue staining assay and regrowth delay experiment after X-Ray irradiation (10Gy), respectively.

Results

The administration of As_2O_3 increases significantly the pO_2 (measured by EPR) in TLT and LLC tumors, an effect that was not observed for the control group. The results were confirmed by ^{19}F NMR relaxometry. The increase in pO_2 induced by As_2O_3 was not due to an increase in tumor perfusion as shown by the Patent blue staining assay. As the increase in pO_2 was not due to an increase in perfusion, the tumor oxygen consumption was investigated. The administration of As_2O_3 significantly decreased the rate of oxygen consumption. Finally, the irradiation (10Gy) of tumors showed a regrowth delay that was significantly increased in arsenic-treated mice.

Conclusion

Arsenic trioxide is an important modulator of pO_2 by decreasing oxygen consumption and enhances the response of tumors to radiotherapy. The time-window for the radiosensitization effect by As_2O_3 can be predicted using MR oximetry techniques (EPR or ^{19}F NMR relaxometry)

References (1) Gallez et al, NMR Biomed. 2004, 17,240-262. (2) Jordan et al, MRM 2009, 61, 634-638.

COMPARISON OF METHODS TO MEASURE OXYGEN CONSUMPTION IN TUMORS CELLS IN VITRO

Caroline Diepart[1], Julien Verrax[2], Pedro Buc Calderon[2], Olivier Feron[3], Bénédicte F.Jordan[1], and Bernard Gallez[1]

1: Louvain Drug Research Institute, Laboratory of Biomedical Magnetic Resonance, Université catholique de Louvain, Avenue Mounier 73, B-1200 Brussels, Belgium
2: Louvain Drug Research Institute, Laboratory of Pharmacokinetics, Metabolism, Nutrition and Toxicology, Université catholique de Louvain, Avenue Mounier 73, B-1200 Brussels, Belgium
3: Laboratory of Pharmacotherapy, Université catholique de Louvain, Avenue Mounier 52, B-1200 Brussels, Belgium

Introduction
The oxygen consumption rate of tumor cells affects tumor oxygenation and response to therapies. Highly sensitive methods of determining cellular oxygen consumption are therefore needed to identify treatments that can modulate this parameter. We compared the performance of three different methods of measuring cellular oxygen consumption: Electron paramagnetic resonance (EPR) oximetry, the Clark electrode, and the Mito Xpress-Xtra fluorescent assay.
Material and methods
We used K562 cells in the presence of rotenone and hydrocortisone, compounds that are known to inhibit the mitochondrial electron transport chain to different extents.
Results
The EPR method was the only method that could identify both rotenone and hydrocortisone as inhibitors of tumor cell oxygen consumption. The Clark electrode and the fluorescence assay demonstrated a significant decrease in cellular oxygen consumption after administration of the most potent inhibitor (rotenone), but failed to show any significant effect of hydrocortisone.
Conclusions
EPR oximetry is, therefore, the most sensitive method of identifying inhibitors of oxygen consumption on cell assays, while the Clark electrode offers the unique opportunity to add external compounds during experiments, and still shows great sensitivity in studying enzyme and chemical reactions that consume oxygen (non-cell assays). Finally, the Mito Xpress-Xtra fluorescent assay has the advantage of a high-sample throughput and low bulk requirements, but at the cost of a lower sensitivity.

Metabolic Stability of Cyclic Nitrone Adducts with $O_2^{\cdot-}$ And $^{\cdot}OH$ Towards Rat Liver Microsomes and Cytosol: a Stopped-Flow ESR Spectroscopy Study

Authors: Nicolas Bézière, Yves Frapart, Antal Rockenbauer, Jean-Luc Boucher, Daniel Mansuy, Fabienne Peyrot

Adress : N. Bézière
UMR 8601 CNRS
45 rue des Saints Pères
75270 Paris cedex 06 - France
Tel: +33 (0)1 42 86 43 64
nicolas.beziere@free.fr

Abstract: The metabolic stability of the spin-adducts derived from reaction of superoxide and hydroxyl radicals with the nitrone spin-trap, 5-*tert*-butoxycarbonyl-5-methyl-1-pyrroline N-oxide (BocMPO), in the presence of rat liver microsomes (RLM) and cytosol, was studied by using a stopped-flow device coupled to an electron spin resonance (ESR) spectrometer. The kinetics of disappearance of the BocMPO-OH spin-adduct and even of the short-lived BocMPO-OOH radical could be followed by ESR spectroscopy with the treatment of the ESR data by an appropriate computer program. The presence of cytosol led to a 50-fold decrease of the half-life of BocMPO-OOH radical, with the intermediate formation of BocMPO-OH. This effect of cytosol was due to an ascorbate- and thiols-dependent reduction of BocMPO-OOH. Rat liver cytosol only led to a 5-fold decrease of the half-life of BocMPO-OH, that was mainly due to cytosolic ascorbate. RLM led to a 10-fold decrease of the BocMPO-OOH half-life because of a direct reaction of the hydroperoxide function of BocMPO-OOH with cytochrome P450 Fe(III). Other ferric hemeproteins, such as metHb and HRP, as well as hemin itself, exhibited a similar behaviour. RLM without NADPH and metHb showed a much weaker effect on BocMPO-OH half-life (2-fold decrease), and RLM in the presence of NADPH caused a greater decrease of the BocMPO-OH half-life (~5-fold). The RLM alone-dependant effect was mainly due to a direct reaction with microsomal P450, whereas the RLM- and NADPH-dependent effect was catalyzed by cytochrome P450 reductase. These first data on the effect of liver sub-cellular fractions on the half-life of the BocMPO-OOH and the BocMPO-OH spin-adducts and on the metabolic pathways involved highlights the importance of the role of heme as a biological cofactor involved in the disappearance of such spin-adducts. They should be helpful for the design of new spin-traps that would form spin-adducts more metabolically stable *in vitro* and *in vivo*.

ASSESSMENT OF MELANOMA EXTENT AND MELANOMA METASTASES INVASION BY USING ELECTRON PARAMAGNETIC RESONANCE AND BIOLUMINESCENCE IMAGING

Q. Godechal[1], F. Defresne[2], P. Levêque[1], J-F. Baurain[3], O. Feron[2], and B. Gallez[1]

[1]Biomedical Magnetic Resonance Unit, Université Catholique de Louvain, Av. Mounier 7340, 1200 Bruxelles, Belgium
[2]Pharmacotherapy Unit, Université Catholique de Louvain, Bruxelles, Av. Mounier 54, 1200 Bruxelles, Belgium
[3]Medical Oncology Unit, Université Catholique de Louvain, Av. Hippocrate 5471, 1200 Bruxelles, Belgium.

Introduction

Malignant melanoma is a skin tumor characterized by the uncontrolled proliferation of melanocytes, which can lead to metastasis mainly in lungs. The incidence of melanoma is rising each year. Nowadays, the cumulative lifetime risk for an invasive melanoma is estimated at 1/59 in the U.S. For this reason, it is essential to develop new effective methods able to detect melanoma. We demonstrated previously that melanin pigments from melanoma tumors can be imaged used an EPR-based method (1).

The purpose of the present study was to assess the ability of EPR to detect and measure the colonization of lungs by melanoma metastases. In order to validate our method, the EPR results were compared with those obtained with bioluminescence imaging (BLI) (2) in a melanoma B16 model with cells transfected with luciferase.

Materials and methods

18 C57/BL6 mice were injected intravenously with 750.000 B16 melanoma cells. After 6, 15 and 18 days, mice were measured *in-vivo* with bioluminescence (Xenogen), the lungs were then excised, freeze-dried and measured by X-band EPR spectroscopy and imaging with a Bruker Elexsys spectrometer.

Results

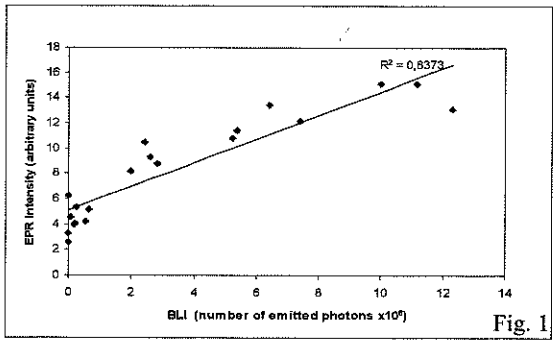

Fig. 1

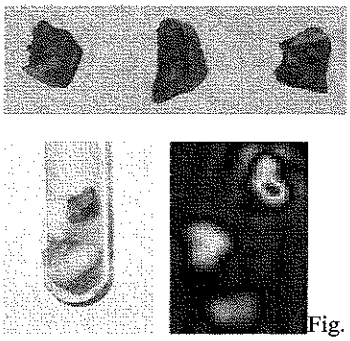

Fig. 2

We observed a linear progression of the EPR and BLI intensities, corresponding to the progression of tumor invasion. As shown in the figure 1, a strong correlation (R^2 = 0.8373) between the results obtained with EPR and the results obtained with BLI is observed. EPR spectroscopy was found to be more sensitive than BLI, and able to detect tiny quantities of melanin (2 µg). As shown in figure 2, EPR imaging, used as a tool to confirm the EPR results, also demonstrated the convenience of EPR to quantify the melanoma invasion inside the lungs.

Discussion and conclusion

We used for the first time EPR as a tool to quantify the melanin content of melanoma lung metastasis. To confirm our results, we compared them to results obtained by bioluminescence and showed an excellent correlation. Furthermore, this new method is far more sensitive than BLI and suits for every pigmented melanoma.

References

1. Vanea et al. NMR Biomed. 2008 Mar; 21(3):296-300.
2. Craft et al. J Invest Dermatol. 2005; 125: 159-65.

CAPTOPRIL AND S-NITROSOCAPTOPRIL AS POTENT RADIOSENSITIZERS: COMPARATIVE MR STUDY AND UNDERLYING MECHANISMS.

Bénédicte F. Jordan, Julie Peeterbroeck, Oussama Karroum, Caroline Diepart, Julie Magat, Vincent Grégoire and Bernard Gallez.
Biomedical magnetic resonance Unit, Louvain Drug Research Institute,
Université Catholique de Louvain, Brussels, Belgium.

Purpose: Hypoxia and blood flow heterogeneities are major obstacles for therapy of solid tumors. Many 'provascular' agents have been considered for transiently increasing tumor oxygenation or open the vascular bed in order to sensitize tumors to radiation or chemotherapy. In this context, NO-mediated treatments have been characterized with success as radiosensitizers. In this study, S-nitrosocaptopril (SNOCap), a converting enzyme inhibitor with vasodilatory properties combined to a nitric oxide donor was studied for its effects on tumor hemodynamics using 19F-MRI and EPR oximetry, and compared with captopril.

Material:

TLT (transplantable tumor model) bearing mice were injected IP with either captopril (0.046 mmol/kg in saline), SNOCap (0.046 mmol/kg in ethanol/saline (1/9)), or vehicles. Local pO_2 was estimated using EPR oximetry, and ^{19}F-MRI pO_2 maps were generated. Changes in blood flow were probed by patent blue staining and the rate of oxygen consumption was measured using high frequency EPR. Finally, the therapeutic relevance was evaluated using a single radiation dose of 10Gy of X-rays.

Results:

SNOCap significantly modified tumor pO_2 from 30 to 60 minutes post injection as showed by EPR oximetry, contrarily to captopril (Fig.1). The effect of S-nitrosocaptopril was confirmed by 19F-MRI. Both treatments were able to significantly increase tumor blood flow to the same extent as shown by patent blue staining. A significant decrease in oxygen consumption by tumor cells (factor of 1.4) after S-nitrosocaptopril injection was observed using EPR, but not with captopril alone (Fig.2). Consequently, the administration of S-nitrosocaptopril contributed to the increase in efficacy of radiation therapy with 10Gy of X-rays, an effect that was not observed with captopril alone.

Fig.1

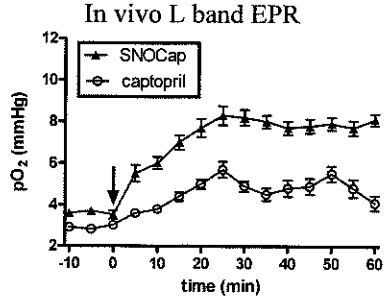

Fig.2 Ex vivo X-band EPR

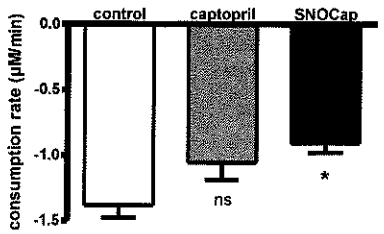

Conclusions:

We identified a time window during which tumor oxygenation was improved, as a result of a combined effect on tumor blood flow and oxygen consumption rate. MR oximetry techniques (EPR and ^{19}F relaxometry) may therefore help in defining the time window for the irradiation after S-nitrosocaptopril administration.

Monitoring Alzheimer amyloid peptide aggregation by EPR

I. Sepkhanova[a], M.H. Shabestari[a], M. Drescher[a], N.J. Meeuwenoord[b], R.W.A.L. Limpens[c], R.I. Koning[c], D.V. Filippov[b], M. Huber[a*]

[a]Department of Molecular Physics, Huygens Laboratory, Leiden University, P.O. Box 9504, 2300RA Leiden, The Netherlands. email*: mhuber@molphys.leidenuniv.nl
[b]Leiden Institue of Chemistry, Leiden University, Leiden, The Netherlands
[c]Leiden University Medical Center, Department of Molecular Cell Biology, Section Electron Microscopy, Leiden, The Netherlands

The aggregation of the β-Amyloid (Aβ) peptide into fibrils and plaques is the chief indicator of Alzheimer's disease. Specific interest in oligomers stems from the suggestion that small, oligomeric aggregates and protofibrils, rather than fully formed fibrils could be responsible for the toxicity of the Aβ-peptide. We investigate the potential of EPR to detect early stages of the aggregation of the Aβ-peptide. We have labeled the 40 residue Aβ peptide variant containing N-terminal cystein (cys-Aβ) with the MTSL (1-Oxyl-2,2,5,5-Tetramethyl-Δ-Pyrroline-3-Methyl) Methanethiosulfonate spin label (SL- Aβ). Fibril-formation in solution of pure SL- Aβ and of SL- Aβ mixed with Aβ was shown by Congo-red binding and electron microscopy. Continuous wave, 9 GHz EPR reveals three fractions of different spin-label mobility. One attributed to monomeric Aβ, one to a multimer (8 to 15 monomers), and the last one to larger aggregates or fibrils. The approach allows detection of oligomers on the timescale of aggregation.

EPR STUDY OF THE EFFECT OF SORAFENIB ON TUMOR HEMODYNAMICS: POTENTIAL USE AS A CO-TREATMENT FOR RADIATION THERAPY.

Oussama Karroum, Vincent Grégoire, Bernard Gallez, and Bénédicte F. Jordan.
Biomedical magnetic resonance Unit, Louvain Drug Research Institute,
Université Catholique de Louvain, Brussels, Belgium.

Introduction

It is well recognized that tumor hypoxia is a critical determinant for radiotherapy and chemotherapy response. FTI's (Farnesyl Transferase Inhibitors) have been shown to be able to modulate pO_2 in experimental tumors (1) and the inhibition of activated Ras has been suggested as a potential method for radiosensitization (2). In the current study, the acute and chronic effects of the Raf inhibitor (=Ras effector), Sorafenib, were monitored *in vivo* using EPR oximetry in experimental tumors and the window of reoxygenation was exploited in order to sensitize tumors to irradiation.

Subject and Methods

FSa II (Fibrosarcoma) bearing C3H mice were injected daily with either Sorafenib (45mg/kg/day,IP) or vehicle. Local pO_2 was estimated using in vivo EPR oximetry. The therapeutic relevance was assessed by measuring regrowth delays after irradiation with 20 Gy of X-rays. Changes in blood flow were probed by patent blue staining and O2 consumption was measured using ex vivo X-Band EPR.

Results

Sorafenib dramatically modified FSaII tumor pO_2 upon one day post-injection and the effect was prolonged until day 4, with a peak at days 2-3 (Fig.1). This window of reoxygenation (day 2) was used for the rest of the experiments: (i) a rough estimate of tumor blood flow showed a significant increase compared to control tumors; (ii) oxygen consumption decreased in treated tumors (Fig.2); (iii) the tumor radiosensitivity was enhanced by a factor of 1.5 compared to X-rays 'alone'; (Fig.3).

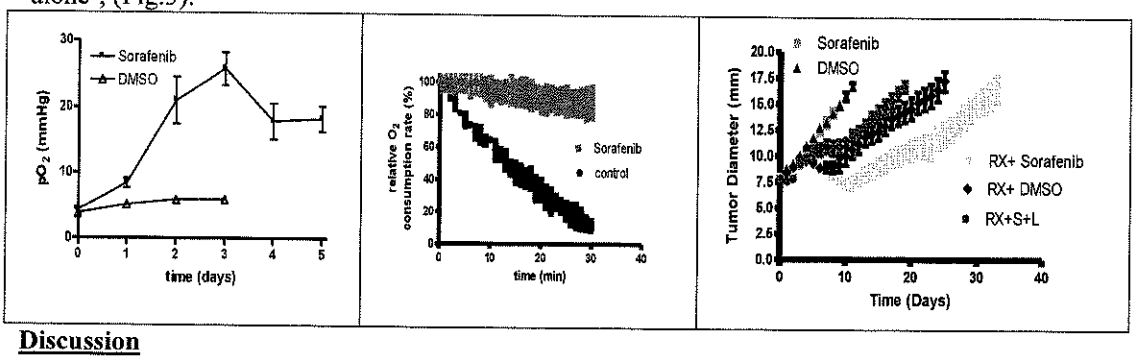

Discussion

In vivo EPR oximetry allowed the identification of a window of reoxygenation in FSaII experimental tumors following administration of Sorafenib, which was further successfully exploited for improving radiation response. The increase in tumor oxygenation was shown to be the result of two major factors: (i) an increase in blood flow, which could be explained by one of the numerous target of Sorafenib, such as CRAF, VEGFR-2, VEGFR-3 and PDGFR-ß, that are all implicated in tumor vascularisation; and (ii) the decrease of oxygen consumption in treated tumors, likely to be due to its action on GSH depletion and mitochondrial respiratory chain (cytochrome c) (3).

References:
(1) Cancer research. 2001. 61. 2289-2293.
(2) Int J Radiat Biol. 2003;79:569-76.
(3) Cancer Biology and Therapy, 2009. 8:1904-1913.

Intrinsic Si dangling bond defects at the (110)Si/SiO_2 interface

K. Keunen, A. Stesmans, and V. V. Afanas'ev
Semiconductor Physics Laborator,
Department of Physics and Astronomy, University of Leuven

Conventional electrical devices have traditionally been fabricated on Si substrates with a (100) crystalline face orientation, owing to their high electron mobility and reduced inherent interface trap density D_{it}. However, further scaling of the conventional Si metal-oxide-semiconductor field effect transistor (MOSFET) is reaching its limits. With the introduction of new device structures that can easily be fabricated outside the traditional (100) plane, such as vertical MOSFET and multigate (e.g., FinFET) devices, renewed interest has been sparked in the application of alternative surface orientations such as (111) and (110) to optimize the performance of electrical devices. This is especially directed to the (110) Si face as this shows a much enhanced hole mobility as compared to the (100) orientation, up to more than a factor of two.

An electron spin resonance study of the quality of the (110)Si/SiO_2 interface in terms of inherent defect density as a function of oxidation temperature (T_{ox}) has been carried out in the range T_{ox} = 200-1050 °C. Only one type of interface defect is observed, closely related to P_b and P_{b0} observed for (111) and (100)Si, respectively. First accurate g matrix determination has been carried out, yielding $g_{//}$ = 2.0018±0.0001 and $g_{\perp}$= 2.0082±0.0001, closely coinciding with those of P_{b0}, upon which the defect is named $P_{b0}^{(110)}$.

While at low T_{ox} a very high density of $P_{b0}^{(110)}$ defects (~ 8 ×10^{12} cm^{-2}) is observed, the density gradually decreases for T_{ox} above ~ 600 °C. This indicates the SiO_2 oxide layer to undergo a global structure relaxation, initiating at ~600 °C. This stress release effect is also signaled by a decrease in line width at $T_{ox} \approx$ 600 °C and a change in line shape asymmetry with increasing T_{ox}. A small change of principal g matrix values can also be explained in this view. In contrast with inferred interface trap densities from previous electrical measurements the quality of the (110)Si/SiO_2 interface is found to be the worst compared to the more conventional (111) and (100) faces.

EXPERIMENTAL DETERMINATION OF THE RELATIVE RADIAL DOSE DISTRIBUTION IN HIGH GRADIENT REGIONS AROUND IRIDIUM-192 WIRE SOURCE. COMPARISON BETWEEN ELECTRON PARAMAGNETIC RESONANCE IMAGING, GAFCHROMIC EBT FILM DOSIMETRY AND MONTE CARLO SIMULATIONS

N. Kolbun[a], P. Levêque[a], F. Abboud[b], S. Vynckier[b], and B. Gallez[a]
[a]Biomedical Magnetic Resonance Unit, Louvain Drug Research Institute, Université catholique de Louvain, Brussels, Belgium, [b]Molecular Imaging and Experimental Radiotherapy Unit, Université catholique de Louvain, Brussels, Belgium

The experimental determination of doses at proximal distances from radioactive sources is difficult because of the steepness of the dose gradient. The goal of this study was to determine the relative radial dose distribution for a low dose rate (LDR) Iridium-192 wire source using Electron Paramagnetic Resonance Imaging (EPRI) technique and to compare the results obtained with Gafchromic EBT film dosimetry and Monte-Carlo simulations.
Lithium formate and ammonium formate were chosen as an EPR dosimetric material. The dose distribution was assessed by EPRI of the radiation induced stable free radicals in the lithium formate and ammonium formate phantoms. EBT films were also inserted inside ammonium formate phantoms for comparison. Monte Carlo (MC) simulation was done using MCNP4C2 software code.
The spectrum shape of the irradiated ammonium formate represents a single narrow EPR line. Each reconstructed 2D EPR image reflects the known shape of phantoms. The color code directly depicts the radial dose distribution around the radioactive wire source, as shown in Fig.1. The spatial resolution of 2D EPR images was enhanced by a factor of 2.2, using ammonium formate, because of its linewidth, which was about 0.75 mT narrower than that of lithium formate. The spatial resolution was also amplified by increasing the magnetic field gradient from 250 mT/m to 450 mT/m by a factor of 1.8. For 2D EPR images with a low signal to noise ratio and a high magnetic field gradient it was useful to apply a Gaussian filter. The results of EPRI data are consistent with those of Gafchromic EBT films and MC simulations at distances from 1 to 2.9 mm within 1%. The radial dose values obtained by EPRI were lower about 4% at distances from 2.9 to 4 mm than those determined by MC and EBT film dosimetry. The radial dose gradient from the source out to 2 mm is still steep, it decreases up to 45%, while levels off more smoothly from 2 mm to 3 mm up to 28% (Fig.2).

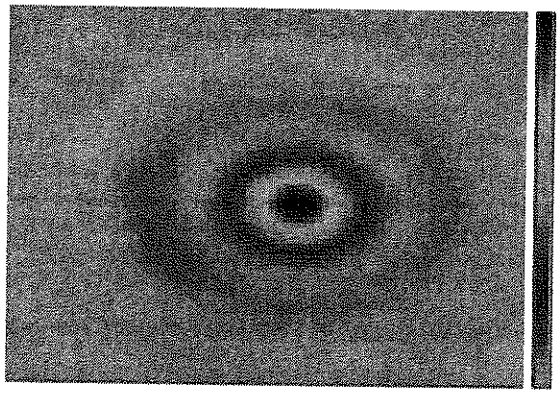

Fig. 1 2D EPR image of ammonium formate phantom irradiated by ^{192}Ir wire source
white boxes

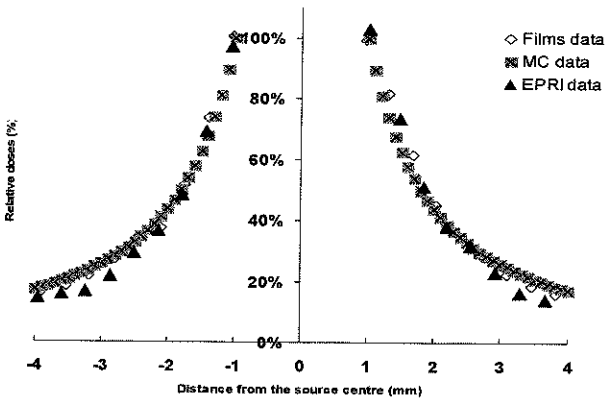

Fig.2 Radial dose profiles, EPRI data, black triangles, MC calculations, grey squares, EBT film results,

Ammonium formate is a suitable material for application in brachytherapy dosimetry using EPRI. EPRI technique allows the estimation of the relative radial dose distribution at short distances for a ^{192}Iridium wire source. In this study, we developed 2D EPRI dosimetry for validation and comparison with MC simulations, three-dimensional dosimetry can be achievable with the EPR imaging procedure in future.

Radical mechanisms in nitrosamine and nitrosamide-induced whole genome gene expression modulations in Caco-2 cells

Dennie G.A.J. Hebels, Jacob J. Briedé, Roongnapa Khampang, Jos C.S. Kleinjans, Theo M.C.M. de Kok

Department of Health Risk Analysis and Toxicology, Faculty of Health, Medicine and Life Sciences, Maastricht University, PO Box 616, 6200 MD Maastricht, The Netherlands

Abstract

N-nitroso compounds (NOC) may be implicated in human colon carcinogenesis, but the toxicological mechanisms involved have not been elucidated. Since it was previously demonstrated that nitrosamines and nitrosamides, representing two classes of NOC, induce distinct gene expression effects in colon cells that are particularly related to oxidative stress, we hypothesized that different radical mechanisms are involved. Using ESR spectroscopy, we investigated radical generating properties of genotoxic NOC concentrations in human colon adenocarcinoma cells (Caco-2). Cells were exposed to nitrosamides (N-methyl-N'-nitro-N-nitrosoguanidine, N-methyl-N-nitrosurea) or nitrosamines (N-nitrosodiethylamine, N-nitrosodimethylamine, N-nitrosopiperidine, N-nitrosopyrrolidine). Nitrosamines caused formation of reactive oxygen species (ROS) and carbon centered radicals which were further stimulated in presence of Caco-2 cells. N-methyl-N-nitrosurea exposure resulted in a small ROS signal, and formation of nitrogen centered radicals (NCR), also stimulated by Caco-2 cells. N-methyl-N'-nitro-N-nitrosoguanidine did not cause radical formation at genotoxic concentrations, but at increased exposure levels, both ROS and NCR formation was observed. By associating gene expression patterns with ROS formation, several cellular processes responding to nitrosamine exposure were identified, including apoptosis, cell cycle blockage, DNA repair and oxidative stress. These findings suggest that following NOC exposure in Caco-2 cells, ROS formation plays an important role in deregulation of gene expression patterns which are relevant for the process of chemical carcinogenesis in the human colon in addition to the role of DNA alkylation.

POTENTIAL ROLE FOR PGE1 AS A RADIOSENSITIZER: EVALUATION OF THE EFFECT ON TUMOR OXYGENATION USING IN VIVO EPR OXYMETRY

Pierre Danhier, Julie Magat, Oussama Karroum Bénédicte F. Jordan, and Bernard Gallez.
Biomedical magnetic resonance Unit, Louvain Drug Research Institute,
Laboratory of Molecular Imaging and Experimental Radiotherapy;
Université Catholique de Louvain, Brussels, Belgium.

The aim of this study is based on the hypothesis that some molecules may enhance tumor radiosensitivity by increasing tumor pO_2. The prostaglandin PGE_1 is currently used for its vasodilatator properties to treat erectile dysfunction. The drug is also used in newborn babies with congenital heart defects to maintain the patency of the ductus arteriosus. Our hypothesis is that PGE_1 could also improve tumor blood flow and thus the tumor pO_2. Indeed, it was already reported that PGE_1 decreased tumoral interstitial pressure, wich is an important obstacle to tumor perfusion (1).

The effect of PGE_1 (25µg in intratumoral injection, IT) was assessed on NMRI mice bearing Transplantable Liver Tumors (TLT). Local pO_2 was measured using L-Band EPR and pO_2 mapping was performed with ^{19}F relaxometry.

Our first results showed that tumor pO_2 increases after intratumoral injection of PGE_1. These results are confirmed by EPR (figure 1) and ^{19}F techniques . At the maximum pO_2, a rough estimate of tumor perfusion, assessed by Patent Blue Staining, showed that tumor blood flow is enhanced in PGE_1 group compared to control group.

In conclusion, PGE_1 increases tumor oxygenation thanks to the vasomotor properties of the drug. The next step is now to perform a regrowth delay assay in order to assess the therapeutic relevance of the drug.

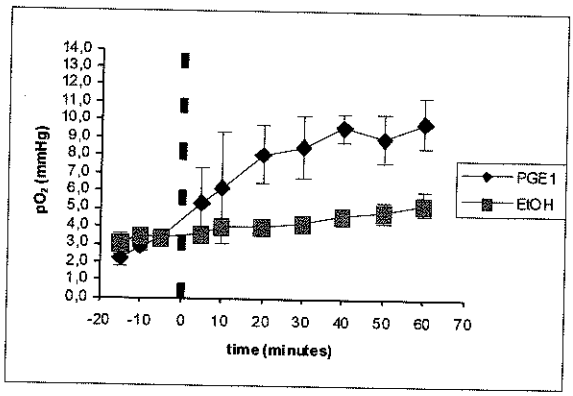

Fig 1 : **EPR L-band results**

References:

(1) FASEB J., 17(12), 1756-8

EPR of the Cyanide Adducts of Protoglobin Mutants

Filip Desmet*, Lesley Tillemans**, Alessandra Pesce#, Marco Nardini%, Martino Bolgnesi%, Luc Moens**, Sylvia Dewilde**, Sabine Van Doorslaer*
University of Antwerp, *Departments of Physics and **Biomedical Sciences, Belgium
%University of Milano, Department of Biomolecular Sciences and Biotechnology, Italy
#University of Genova, Department of Physics, Genova, Italy

Vertebrate hemoglobin and myoglobin are two well known members of the globinfamily. These heme-proteins are best known for their O2 transport function, this function is however a fairly recent adaptation. The more ancient functions of members of the globin family, which are found in all kingdoms of life, are related to oxygen sensing and enzymatic activity. Indeed, globin-coupled sensor proteins are found in many bacteria. It has been suggested that a group of single domain globins, the socalled protoglobins, which are found in more primitive organisms, are the evolutionary predecessor of these sensor-proteins, although this point is still being debated.

We present here the results of our EPR investigation of the cyanide-bound form of MaPgb, the protoglobin of the bacterium Methanosarcina acetivorans. This protein has a number of unique features that make it stand out from all the other characterised members of the globin family. MaPgb is the only known globin to have a higher affinity for O2 than for CO. The X-ray structure of this protein has revealed a system of two tunnels leading to the ligand binding site at the heme, together with an N-terminal tail of 20 amino-acids that folds back to the heme-cofactor at the centre of the protein. A number of point-mutants of this protein were expressed to investigate the function of this tunnel system.

The X-ray structure of the as purified form of the protein showed the presence of an unidentifiable ligand in the heme pocket of the mutants. To remove any doubt about the nature of the distal ligand it was decided to study the cyanide-bound form of the proteins. Cyanide is a very strong ligand of heme proteins in the Fe(III) form. The addition of cyanide to the protein solution is thus an effective way to remove any doubt about the ligation of the protein.

The CW-EPR investigation of the cyano-met form of the MaPgb mutants showed low gmax-values (≤ 3) for all of the mutants. This is surprising within the globin family where the cyano-met forms have EPR signals which are typically of the large gmax type. This prompted us to perform pulsed EPR experiments.

Various factors such as distortions of the heme plane, deprotonation of the proximal histidine and the orientation of the ligands may affect the anisotropy of the g-values and other parameters of the spin Hamiltonian. We combine our EPR data with the X-ray structures of the various cyanide ligated MaPgb mutants to find the origin of the low gtensor anisotropy.

List of participants

Callens Freddy	UGent	freddy.callens@ugent.be
Lauwaert Johan	UGent	johan.lauwaert@ugent.be
Sakhabutdinova Nuriya	UGent	Nuriya.Sakhabutdinova@UGent.be
Vrielinck Henk	UGent	Henk.Vrielinck@UGent.be
Tarpan Mihaela Adeluta	UGent	mihaelaadeluta.tarpan@ugent.be
Zverev Dmitry	UGent	Dmitry.Zverev@ugent.be
Grammenos Angeliki	Université de Liège	
Guelluy Pierre-Henri	Université de Liège	phguelluy@ulg.ac.be
Hoebeke Maryse	Université de Liège	M.Hoebeke@ulg.ac.be
Mouithys Ange	Université de Liège	amouithys@ulg.ac.be
Briede Jacco	Maastricht University	J.Briede@GRAT.unimaas.nl
Wijnands KAP.	Maastricht University	N.Wijnands@AH.unimaas.nl
Alejandro Gabriela	University of Antwerpen	gabrialejandro@gmail.com
Cambre Sofie	University of Antwerpen	sofie.cambre@ua.ac.be
Desmet Filip	University of Antwerpen	filip.desmet@ua.ac.be
Ezhevskaya Maria.	University of Antwerpen	Maria.Ezhevskaya@ua.ac.be
González Juan-Carlos	University of Antwerpen	
Goovaerts Etienne	University of Antwerpen	Etienne.Goovaerts@ua.ac.be
Moons Hans	University of Antwerpen	hans.moons@ua.ac.be
Sepideh Zamani	University of Antwerpen	Sepideh.Zamani@ua.ac.be
Van Doorslaer Sabine	University of Antwerpen	sabine.vandoorslaer@ua.ac.be
Vinck Evi	University of Antwerpen	Evi.Vinck@ua.ac.be
Yun Ling	University of Antwerpen	Yun.Ling@ua.ac.be
Teughels Stephanie	PEPRIC	Stephanie.Teughels@pepric.com
Vaes Peter	PEPRIC	Peter.Vaes@pepric.com
Danhier Pierre	UCLouvain	Pierre.danhier@uclouvain.be
Diepart Caroline	UCLouvain	Caroline.diepart@uclouvain.be
Driesschaert Benoit	UCLouvain	benoit.driesschaert@uclouvain.be
Fruytier Anne-Catherine	UCLouvain	Anne-catherine.fruytier@uclouvain.be
Gallez Bernard	UCLouvain	Bernard.gallez@uclouvain.be
Godechal Quentin	UCLouvain	Quentin.godechal@uclouvain.be
Jordan Bénédicte	UCLouvain	Benedicte.jordan@uclouvain.be
Karmani Linda	UCLouvain	Linda.karmani@uclouvain.be
Karroum Oussama	UCLouvain	Oussama.karroum@uclouvain.be
Leprince Julian	UCLouvain	Julian.leprince@uclouvain.be
Leveque Philippe	UCLouvain	Philippe.leveque@uclouvain.be
Lobysheva Irina	UCLouvain	irina.lobysheva@uclouvain.be
Magat Julie	UCLouvain	Julie.magat@uclouvain.be
Marchand Jacqueline	UCLouvain	Jacqueline.marchand@uclouvain.be
Moray Michael	UCLouvain	Michael.moray@uclouvain.be
Radermacher Kim	UCLouvain	Kim.radermacher@uclouvain.be
Veriter Sophie	UCLouvain	sophie.veriter@uclouvain.be
Blok, Huib	University of Leiden	huib@molphys.leidenuniv.nl
Gast, Peter	University of Leiden	gast@molphys.leidenuniv.nl
Groenen Edgar	University of Leiden	egroenen@molphys.leidenuniv.nl
Huber, Martina	University of Leiden	mhuber@molphys.leidenuniv.nl
Mathies, Jennifer	University of Leiden	mathies@molphys.leidenuniv.nl
Shabestari, Maryam	University of Leiden	shabestari@molphys.leidenuniv.nl
Son, Martin van	University of Leiden	son@molphys.leidenuniv.nl
Sottini, Silvia	University of Leiden	sottini@molphys.leidenuniv.nl
Stellinga, Daan	University of Leiden	stellinga@molphys.leidenuniv.nl
Vlaar, Shannon	University of Leiden	vlaar@molphys.leidenuniv.nl

Duc Nguyen	KULeuven	
Stesmans Andre	KULeuven	andre.stesmans@fys.kuleuven.be
Beziere Nicolas	Université Paris Descartes	nicolas.beziere@parisdescartes.fr
Frapart Yves-Michel	Université Paris Descartes	yves.frapart@parisdescartes.fr
vanFaassen Ernst	University of Utrecht	E.E.H.vanFaassen@uu.nl
Muller Robert	University of Mons	robert.muller@umons.ac.be
Vander Elst Luce	University of Mons	luce.vanderelst@umh.ac.be
Penders Marc	Bruker	marc.penders@bruker.be